Materials Research Proceedings 54 (2025) 1747-1756 https://doi.org/10.21741/9781644903599-188

Finish milling of polylactide (PLA) 3D-printed parts: Influence of printing pattern and lubrication on final surface roughness

Margaux LORENZONI[1,a *], Laurent SPITAELS[1], Edouard RIVIERE-LORPHEVRE[1], Jérémy ODENT[2], Rachid M'SAOUBI[3,4], Liam CLOËZ[5], Michaël FONTAINE[5] and François DUCOBU[1]

[1]Machine Design and Production Engineering Lab – Research Institute for Materials Science and Engineering, University of Mons, Place du Parc 20, 7000 Mons, Belgium

[2]Laboratory of Polymeric and Composite Materials (LMPC) - Center of Innovation and Research in Materials and Polymers (CIRMAP), University of Mons, Place du Parc 20, 7000 Mons, Belgium

[3]R&D Material and Technology Development, Seco Tools AB, Björnbacksvägen 2, SE-737 82 Fagersta, Sweden

[4]Department of Mechanical Engineering Sciences - Division of Production and Materials Engineering, Lund University, Ole Römers väg 1, SE-221 00 Lund, Sweden

[5]FEMTO-ST Institute - Applied Mechanics Dept., Université de Franche-Comté - SUPMICROTECH - CNRS, Rue de l'épitaphe 24, F-25000 Besançon, France

[a]margaux.lorenzoni@umons.ac.be

Keywords: Polylactide, PLA, Additive Manufacturing, Milling, Finishing, Printing Pattern, Surface Roughness

Abstract. Fused Filament Fabrication (FFF) is an additive manufacturing (AM) process bringing many advantages over conventional processes such as allowing to obtain complex geometries and personalized designs at a lower cost. However, this process does not allow to reach tight surface roughness nor dimensional tolerances. To overcome these limits, post-production finishing techniques are required, such as finish milling. Yet, due to their intrinsic properties, thermoplastics tend to melt and form burr during cutting preventing the reach of fine surface quality. Therefore, this paper proves the relevance and necessity of using lubrication and shortening the machining time to reduce burr formation and allow to reach better final surface roughness.

Introduction

Context. The Material Extrusion (MEX) process is an Additive Manufacturing (AM) technique consisting of building a part by adding successive layers of melted material. MEX has developed quickly since its invention in 1988 [1], overcoming the limitations of traditional manufacturing processes such as machining. 3D-printed parts with complex geometries can therefore be built more rapidly and at a lower cost [1]. Fused Filament Fabrication (FFF) is one of the derivatives of MEX. This process uses polymeric filament as feedstock, therefore providing easy use for private users and industries [2]. With the continuous progress of this production process, applications go from prototyping to production of small series and personalized products [1].

However, limitations persist because of the process nature. Achieving tight dimensional tolerances and fine surface roughness remain a challenge due to the layer by layer building strategy [2]. Consequently, post-processing operations must be studied. Among other post-processes, finish milling appears to be promising. So far, this technique has shown the best dimensional accuracy improvement [3] as well as the best surface finish improvement obtained by a mechanical method

[4]. Moreover, while keeping the advantages provided by the MEX process, machining could be combined inside of a hybrid structure allowing to benefit from the precision of machining [5–8].

Different polymers can be used with the MEX process. However, polymer use could raise ecological concerns as this technology grows, if the materials used cannot be produced and recycled in a responsible manner. To this end, Polylactide or Polylactic acid (PLA) is a bio-sourced candidate of interest, which can be produced from corn, sugar cane, sugar beet, etc. [9]. This polymer can also be recycled in different ways or composted using micro-organisms [10,11].

Regarding its chemical structure, PLA is linear aliphatic polyester based on lactic acid. Its chains contain both hydroxyl and carboxyl groups [11]. This polymer can be produced via two different processes. The first one, conventional polycondensation, produces low molecular weight molecules. The term Polylactic acid will be used to designate PLA produced in this way. The second one is produced by catalytic ring-opening and leads to higher molecular weight polymer, which will be named Polylactide. PLA is constituted of three stereoisomers making it semicrystalline. Molecular weight and polymer architecture (proportion of crystalline and amorphous stereoisomers) define the thermal and mechanical properties of PLA as well as its crystallinity [11].

Literature review and motivation of the study. Because of the interesting characteristics of PLA, several research groups have started to investigate drilling [12] and milling of PLA [3,13–17]. Different milling approaches were studied. While some focus on slot milling [13–15], others have considered pocket [16], profile [3] and shoulder milling [17]. The main points of interest also vary, going from the cutting forces during milling [13] to burr formation [15,16] and, most frequently, to the arithmetic surface roughness (R_a) that can be achieved by machining [3,13–15,17].

Regarding surface roughness, Lalegani Dezaki et al. [3] achieved the best results with an R_a of 0.358 µm. However, the specific milling tools used to achieve this surface quality on complex surfaces are not clearly identified. Pămărac and Petruse [17] also reported low surface roughness, achieving an R_a of 0.6 µm in shoulder milling.

All studies, except for Cloëz et al. [13], used a lubricant during machining to ensure proper chip removal and provide a cooling effect on the material. When specified, pressurized air was used as the lubricant. Cooling liquids are generally avoided due to the lack of information on their interaction with the material and their environmental impact [16]. However, no studies have compared the results of machining with and without lubrication.

Moreover, Dilberoglu et al. [18] emphasize the influence of heat generation during machining of polymeric materials. Unlike metals which are natural conductors, polymers such as PLA are insulators (thermal conductivity λ of 0.12 W/(m.K) for PLA [19] against 237 W/(m.K) for aluminum [20]) and have a high thermal expansion coefficient (between 50 and 200 µm/mK) [21]. Therefore, heat generated during the machining process may not dissipate effectively from the machined zone, potentially causing thermal deformation and/or degradation of the workpiece [21], especially if the glass transition temperature is reached [18]. In addition, Mehtedi et al. [15] draw the conclusion that higher burr formation and heat generation during machining are linked, since the latter can soften the material.

In summary, questions remain about the impact of lubrication on heat management during the machining of PLA. The potential effects of heat rise on surface quality and cutting forces also need to be determined and no study has investigated the potential impact using a milling pattern identical to the printing pattern on the final surface quality. Therefore, the aim of this study is to determine the relevance of using similar printing and machining patterns as well as lubrication (compressed air) to guarantee effective heat dissipation during finish milling of FFF-obtained parts, to ensure low surface roughness of the machined areas and process stability in terms of cutting forces.

Material and Method

Part design and printing. Samples were designed to optimize material consumption and printing time while being able to study and machine their top face. The parts (Fig. 1a) were 10 mm thick with a 30 mm by 30 mm square face.

The samples were printed using a 2.85 mm-diameter filament of Native Nanovia EF 3D850 Polylactide (PLA). Material drying was performed using a SUNLU FilaDryer S2 set to 50°C during 16 hours before printing, reaching a 20% humidity level inside of the drying device.

Thermal properties of the material were determined by Differential Scanning Calorimetry (DSC) using a TA Instruments DSC Q2000. For this test, heating and cooling rates of 10°C/min between -20°C and 210°C were operated. To avoid any thermal history effect, a second scan was performed. Phases transition temperatures were computed as follow and confirmed the values given by the manufacturer [22]:

- Glass transition temperature T_g: 61°C
- Crystallization temperature T_c: 104°C
- Melting temperature T_m: 176°C

An Ultimaker S3 with AA 0.4 mm print cores was used to print the samples. A light mist of 3DLAC adhesive spray was applied on the built plate before each print to avoid samples warping. A modified version of the Balanced Fast printing strategy proposed by the Ultimaker Cura 5.6.0 slicer was chosen. The parameters selected allowed to both match the manufacturer recommendation [22] and reduce printing time since the parts are meant to be finished by milling (Table 1). As one of this study focuses resides on the link between printing patterns and machining trajectories, the number of walls was set to zero to avoid creating a shell effect around the desired pattern on the top and bottom layers (Fig. 1b). Therefore, extra infill walls were added around the infill in the middle layers of the parts (Fig. 1c). These extra infill walls aim to ensure the part rigidity and proper holding during machining.

Table 1 – Printing parameters

Layer height	0.2 mm
Wall thickness	0 mm
Top/Bottom thickness	2 mm
Top/Bottom pattern	Concentric/Lines
Infill density	10%
Infill pattern	Grid
Extra infill wall count	10
Printing temperature	200°C
Build plate temperature	60°C
Print speed	50 mm/s
Fan speed	100%

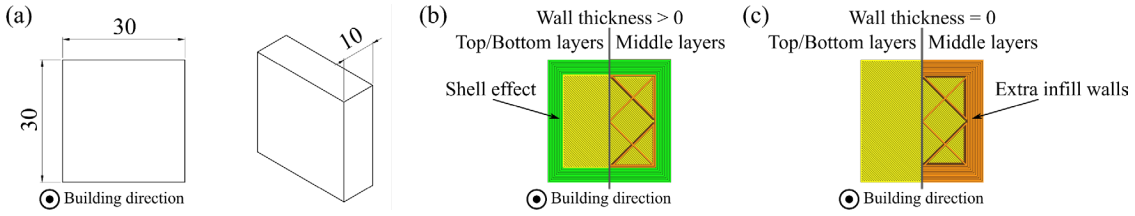

Figure 1 – Design of the parts (in mm) (a), Shell effect (b), and Extra infill walls (c)

Finish milling. Surface finish milling operations were performed on a Mikron VCE 600 Pro. When used, lubrication was in the form of compressed air flow at a 6-bar pressure.

For this study, the 93060-F solid mill from Seco Tools was selected since this tool is specifically designed for thermoplastics. It is characterized by a 6-mm diameter (D), two teeth (Z), and a maximal axial depth of cut $a_{p,max}$ of 20 mm.

The whole surface of the sample was machined using consecutive passes, each of which had an axial depth of cut a_p of 0.5 mm and a radial depth of cut a_e of 3 mm. According to Boschetto et al. [23] recommendation, depths of cut were set to cut through layers rather than between layers. In fact, according to the cited study, depths of cut should be large enough to erase the original morphology of the surface but should not be interfering with the interlayer zone where internal defects and voids can be found. The tool did not show any sign of wear regarding ISO 8688-2 [24] at the end of the experimental tests.

The full experimental set up described in the following sections is presented in Fig. 2.

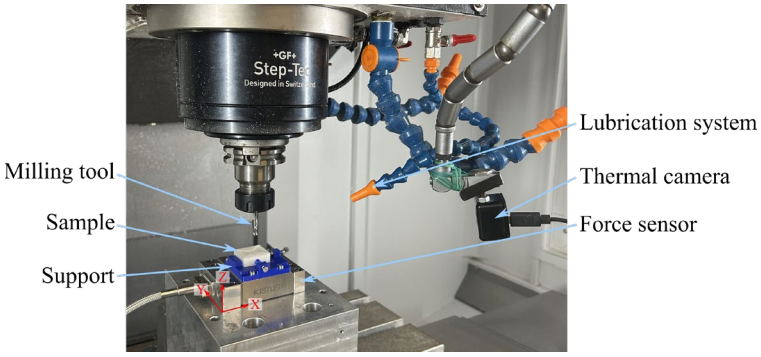

Figure 2 – Experimental setup

Cutting conditions. Machining conditions for this study were selected from literature. The parameters chosen correspond to the ones giving the best results in terms of surface roughness after machining in dry conditions [13]. Therefore, the cutting speed v_c and the feed per tooth f_z were respectively set to 75.4 m/min and 0.1 mm/tooth.

Different cutting patterns were performed (Fig. 3) depending on the printing pattern of the sample. For each printing pattern, a conventional zig machining pattern was used as well as a machining pattern following the printed one. The experimental plan, including three repetitions of the four presented combinations, was carried out twice: once in dry conditions (without any kind of lubrication) and once under pressurized air.

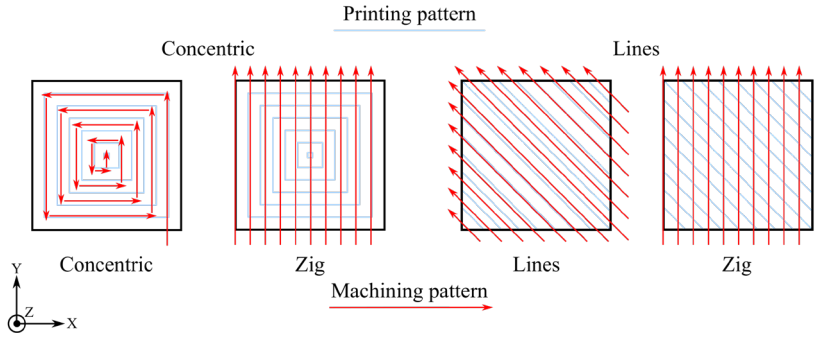

Figure 3 – Printing and machining patterns

Surface roughness. Values of arithmetic surface roughness R_a were assessed following the guidance of ISO 4288 [25] and using a Diavite DH-06 surface roughness meter. Surface roughness was measured before and after machining on the top face of the samples. To best represent the surface quality of the whole face, surface roughness was determined in eight zones of the samples top face. These zones are designated by letters from A to H according to Fig. 4.

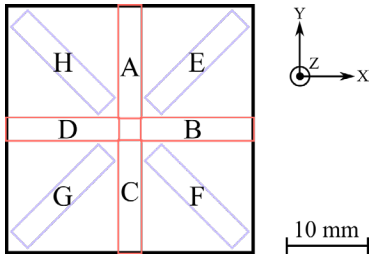

Figure 4 – Zones of surface roughness measurements

Cutting forces. A 3D-printed support was used as a clamping system to hold the parts during machining. The support itself was then attached to a Type 9256C2 Kistler force sensor (Fig. 2). Recordings of the cutting forces signals were acquired using a Kistler 5070A charge amplifier and Kistler 5697A2 data acquisition system, both interfaced with a computer running the DynoWare software. The data was sampled at a frequency of 20 kHz.

Raw data was processed using a Butterworth low pass filter of order 4 with a cutoff frequency of 2500 Hz, which corresponds to half of the natural frequency of the Kistler force sensor. The resulting cutting force F_c RMS value of each pass was then computed from F_x and F_y measured by the force sensor and filtered as described.

As for the machining tests using lubrication, the compressed air contribution on the measured forces was determined by running the machining program three times after a run of effective machining. The average force RMS due to the compressed airflow itself was therefore computed and subtracted from the resulting cutting force F_c RMS.

Temperature monitoring. Temperatures were monitored during milling using an IQ-AAA Seek Thermal camera with a range from 10°C to 300°C. The camera shows a temperature accuracy of 5% within this range according to the manufacturer. The considered emissivity ε for this study was set to 0.78 according to Ferraris et al. [26].

Two forms of the same data were recorded during machining: colored images such as Fig. 5 and CSV files showing numerical values of the recorded temperatures for each pixel of the images. Therefore, the maximum temperature reached for each test could be extracted from the series of CSV files as a first indicator of temperature during the machining tests.

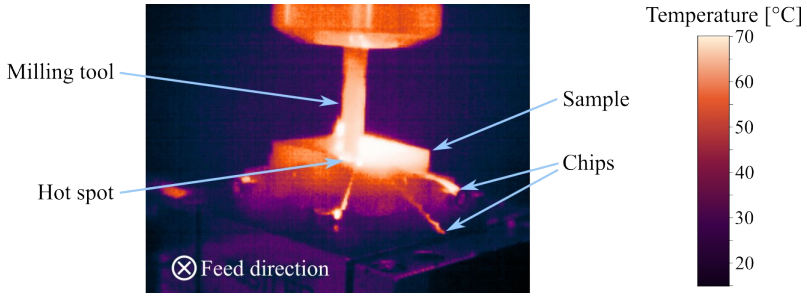

Figure 5 – Thermal camera image

Results and Discussion

Samples visual assessment. A visual examination of the samples was conducted to assess the presence of burrs in different zones of the samples. The affected zones include the entry zone where the tool first enters the sample, the exit zone, and the face of the sample (Fig. 6).

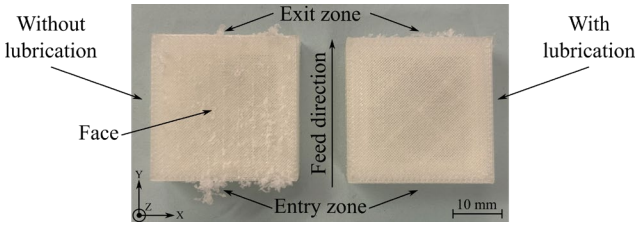

Figure 6 – Burr formation zones (e.g. lines printing pattern and zig strategy)

Exit burr appears almost systematically no matter the cutting conditions. However, when machined under compressed air, the burr is small and very brittle. Unlike exit burr appearing almost consistently, face burr and entry burr is only visible in non-lubricated conditions. In these conditions only, burr formation on the face of the samples prevented from taking roughness measurements after machining. The formation of burr on the samples face may be due to two combined factors: the lack of chip elimination and the temperature increase [18].

Temperature monitoring. The temperature increase, and particularly the reach of temperatures above the glass transition temperature T_g, is mentioned by Dilberoglu et al. [18] as a possible cause for inferior surface quality. The maximum temperatures recorded during machining in this study are shown in Table 2. These temperatures do not vary significantly between the cutting strategies following the printing pattern and the ones not following it.

Table 2 – Maximum machining temperatures

Printing pattern	Machining pattern	With lubrification [°C]	Without lubrification [°C]
Concentric	Zig	75	141
Concentric	Concentric	73	138
Lines	Zig	76	144
Lines	Lines	75	145

On the contrary, maximum machining temperatures decrease notably with the use of compressed air. Although temperatures still reach above the glass transition temperature T_g of PLA (61°C) in the lubricated cases, lubrication can help to lower the potential heat impact and degradation on the polymer. Moreover, in the non-lubricated cases, temperatures recorded during machining rise largely above T_g and T_c (104°C). In other terms, the amorphous phases of PLA reached a high enough temperature to transition from a glassy (rigid and brittle) state to a viscous state. Chains of crystalline stereoisomers were therefore allowed to rearrange into a crystalline and more ordered form increasing the crystallinity of the impacted zones. As for the amorphous stereoisomers chains, they stayed in their viscous state which may be the cause of the poor surface quality obtained in non-lubricated cases. These amorphous phases can no longer be properly cut because of their viscosity and are rather pulled by the tool [27]. However, thanks to the low depth of cut used in this study, cases of permanent chip fusion and wrapping around the tool [16] were avoided despite the high temperatures reached. It should however be noted that material did wrap around the tool briefly on multiple occasions during the machining process in non-lubricated cases. Lastly, because machining temperatures stayed under T_m (176°C), the crystalline phases did not melt, allowing the polymer to remain in solid state and the part to keep its integrity.

Surface roughness analysis. Surface roughness could only be assessed on the samples machined using lubrication. Indeed, as expressed in the visual assessment section, burr formed on the face of the sample when lubrication was not used (Fig. 6). The burr formed during the finishing process was too high to be able to take relevant measurements in terms of arithmetic roughness.

Average surface roughness R_a (over three samples and over the eight zones defined on Fig. 4 for each sample) of parts machined in lubricated conditions decreases significantly compared with the average surface roughness before machining (Fig. 7). For instance, surface roughness goes

from 10.34 µm and 4.55 µm for the concentric and the lines printing patterns respectively to 2.64 µm and 2.50 µm for the same respective printing patterns machined with a zig strategy. Furthermore, machining seems to also significantly decrease dispersion in terms of surface roughness.

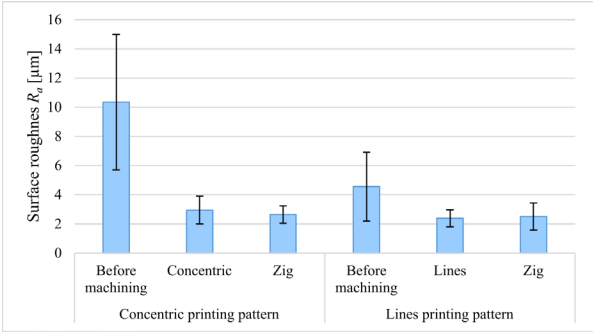

Figure 7 – Mean R_a before and after machining with lubrication

Regarding dispersion before machining, surface roughness of the parts top face is highly dependent on the pattern and the orientation of the surface roughness R_a measure. For instance, the surface roughness measures were compared to the surface roughness classification of ISO 1302 [28], as showed on Fig. 8.

For the concentric pattern faces before machining, R_a is higher than 6.3 µm all over the face and more than doubles on the diagonals F, G, and H. For these parts, although Fig. 8 only showcases two different classes of ISO 1302 [28], the limits between the classes do not follow a linear progression and R_a needs to increase by 6.2 µm to fall into the highest presented class.

Regarding the lines printing pattern, dispersion between the zones is more limited and is mostly due to the fact that measures in F and H zones are taken in the same direction as the lines of the pattern. Surface roughness measurements values are therefore very low, reaching as low as 0.45 µm. These values are, however, not representative of the actual surface quality of the face and this category of low surface roughness could not be reached, even after the finishing operations.

After machining, three different surface roughness classes are reached (Fig. 8). However, these classes cover a smaller interval of values than the ones covered before machining. Surface roughness stays between 1.42 µm and 4.44 µm after machining.

Similarly to the temperature trends, there are no significant differences between surface roughness obtained using a zig strategy or following the printing pattern. Therefore, the strategy requiring less machining time should be preferred, which corresponds to the concentric strategy for this study. Limiting milling time allows to increase productivity while ensuring that the material stays at high temperatures for the least amount of time.

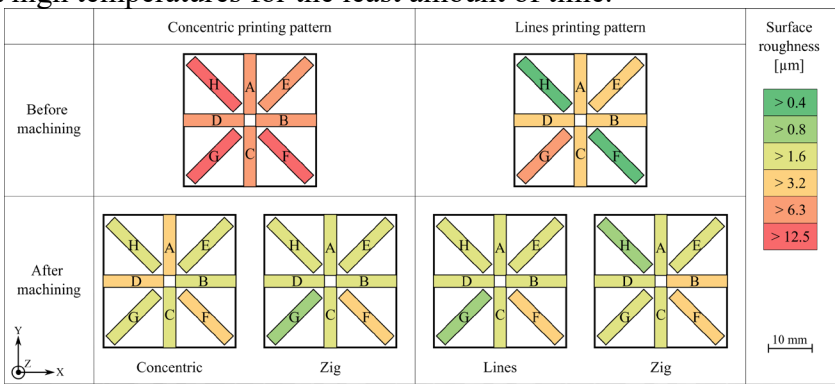

Figure 8 – Comparison of measured surface roughness R_a to the classes of ISO 1302

Cutting forces analysis. Values of the cutting force F_c RMS follow the same trend as the surface roughness and the machining temperatures (Fig. 9). The cutting forces decrease with the use of pressurized air as lubricant. This phenomenon could be linked to the fact that, in lubricated cases, PLA is properly cut and evacuated. Therefore, it does not cause any additional friction by wrapping around the tool or fusing with the parts surface.

The cutting pattern does not seem to have a significant influence on the cutting forces nor on the dispersion. Values of F_c RMS vary between 4.83 and 5.40 N in non-lubricated conditions and between 3.17 and 3.51 N when lubrication is used.

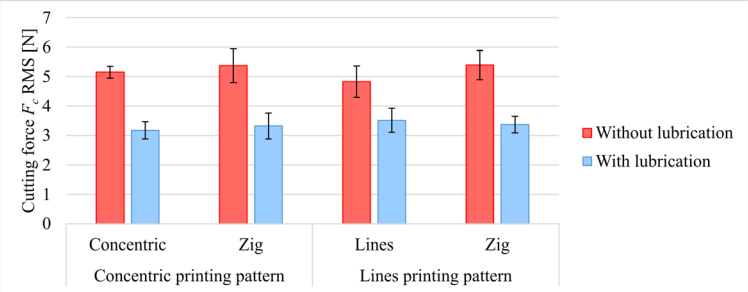

Figure 9 – Cutting force F_c RMS depending on the machining strategy

Conclusion and Prospects

This study has demonstrated the importance of lubrication on the surface finish milling of PLA parts obtained by FFF. Thermal properties of polymers, including low thermal conductivity and low melting temperature, remain a challenge while using milling as a finishing process. Key findings of this study are:

- Lubrication must be used to reach fine surface quality in surface finish milling of PLA parts.
- Lubrication led to decrease temperatures by almost 50% during machining allowing to lower the cutting forces and to avoid potential polymer degradation.
- Finish milling using lubrication allowed to reach more uniform surfaces with arithmetic surface roughness values between 1.42 and 4.44 µm with easily removable exit burr.
- Matching the printing and machining patterns does not have a significant influence on the final surface quality, nor the cutting forces, nor the machining temperature.
- Since the machining pattern does not have a consequential impact on the final surface roughness, the fastest machining strategy, which is the concentric strategy in this study, should be chosen to limit the heat rise and increase productivity.

Acknowledgments

The first author would like to thank Alexander Pizzaro Garcia for his precious help during the experimental campaign.

This work was carried out within the Manufacturing 21 network, which gathers about 20 French research laboratories. The covered topics are the study and modeling of the manufacturing processes, especially machining and additive manufacturing, as well as the emergence of new manufacturing methods.

References

[1] Pei E, Bernard A, Gu D, Klahn C, Monzón M, Petersen M, et al., editors. Springer Handbook of Additive Manufacturing. Cham: Springer International Publishing; 2023. https://doi.org/10.1007/978-3-031-20752-5

[2] Gibson I, Rosen D, Stucker B, Khorasani M. Additive Manufacturing Technologies. Cham: Springer International Publishing; 2021. https://doi.org/10.1007/978-3-030-56127-7

[3] Lalegani Dezaki M, Mohd Ariffin MKA, Ismail MIS. Effects of CNC Machining on Surface Roughness in Fused Deposition Modelling (FDM) Products. Materials 2020;13:2608. https://doi.org/10.3390/ma13112608

[4] Vyavahare S, Teraiya S, Panghal D, Kumar S. Fused deposition modelling: a review. Rapid Prototyp J 2019;26:176–201. https://doi.org/10.1108/RPJ-04-2019-0106

[5] Mertkan İA, Tezel T, Kovan V. Improving surface and dimensional quality with an additive manufacturing-based hybrid technique. Int J Adv Manuf Technol 2023;128:1957–63. https://doi.org/10.1007/s00170-023-12055-z

[6] Susanto B, Rashyid MI, Tanbar F, Ariyadi HM, Muflikhun MA. Surface roughness and dimension accuracy data from hybrid manufacturing process using PLA material. Data Brief 2024;54:110477. https://doi.org/10.1016/j.dib.2024.110477

[7] Lee J, Song J, Lee YC, Kim JT. Development of a huge hybrid 3D-printer based on fused deposition modeling (FDM) incorporated with computer numerical control (CNC) machining for industrial applications. High Temp Mater Process 2022;41:123–31. https://doi.org/10.1515/htmp-2022-0018

[8] Grguraš D, Kramar D. Optimization of Hybrid Manufacturing for Surface Quality, Material Consumption and Productivity Improvement. Stroj Vestn - J Mech Eng 2017;63:567–76. https://doi.org/10.5545/sv-jme.2017.4396

[9] Kalia S, Avérous L. Biodegradable and Biobased Polymers for Environmental and Biomedical Applications. John Wiley & Sons; 2016.

[10] Li Y, Wang S, Qian S, Liu Z, Weng Y, Zhang Y. Depolymerization and Re/Upcycling of Biodegradable PLA Plastics. ACS Omega 2024;9:13509–21. https://doi.org/10.1021/acsomega.3c08674

[11] Bhattacharya M, Reis RL, Correlo V, Boesel L. Material properties of biodegradable polymers. Biodegrad. Polym. Ind. Appl., Elsevier; 2005, p. 336–56. https://doi.org/10.1533/9781845690762.3.336

[12] Lalegani Dezaki M, Mohd Ariffin MKA, Baharuddin BTHT. Experimental Study of Drilling 3D Printed Polylactic Acid (PLA) in FDM Process. In: Dave HK, Davim JP, editors. Fused Depos. Model. Based 3D Print., Cham: Springer International Publishing; 2021, p. 85–106. https://doi.org/10.1007/978-3-030-68024-4_5

[13] Cloëz L, Fontaine M, Gilbin A, Barrière T. Machinability of PLA obtained by injection molding under a dry milling process, 2024, p. 1877–86. https://doi.org/10.21741/9781644903131-208

[14] Lalegani Dezaki M, Mohd Ariffin MKA. Post-processing of FDM 3D-Printed Polylactic Acid Parts by CNC Trimming. In: Dave HK, Davim JP, editors. Fused Depos. Model. Based 3D Print., Cham: Springer International Publishing; 2021, p. 195–212. https://doi.org/10.1007/978-3-030-68024-4_11

[15] Mehtedi ME, Buonadonna P, Carta M, Mohtadi RE, Marongiu G, Loi G, et al. Effects of milling parameters on roughness and burr formation in 3D- printed PLA components. Procedia Comput Sci 2023;217:1560–9. https://doi.org/10.1016/j.procs.2022.12.356

[16] Kartal F, Kaptan A. EXPERIMENTAL DETERMINATION OF THE OPTIMUM CUTTING TOOL FOR CNC MILLING OF 3D PRINTED PLA PARTS. Int J 3D Print Technol Digit Ind 2023;7:150–60. https://doi.org/10.46519/ij3dptdi.1267634

[17] Pămărac RG, Petruse RE. Study Regarding the Optimal Milling Parameters for Finishing 3D Printed Parts from ABS and PLA Materials. Acta Univ Cibiniensis Tech Ser 2018;70:66–72.

[18] Dilberoglu UM, Yaman U, Dolen M. A comprehensive guide to milling techniques for smoothing the surfaces of 3D-printed thermoplastic parts. Rapid Prototyp J 2024;30:1648–62. https://doi.org/10.1108/RPJ-08-2023-0277

[19] Zmeskal O, Marackova L, Lapcikova T, Mencik P, Prikryl R. Thermal properties of samples prepared from polylactic acid by 3D printing. AIP Conf Proc 2020;2305:020022. https://doi.org/10.1063/5.0033857

[20] Zhang A, Li Y. Thermal Conductivity of Aluminum Alloys—A Review. Materials 2023;16:2972. https://doi.org/10.3390/ma16082972

[21] Dessarthe A. Usinage des polymères. Tech Ing 2000. https://doi.org/10.51257/a-v1-bm7426.

[22] Nanovia. Nanovia PLA EF 3D850 : Sans perturbateur endocrinien : Nanovia. Nanovia - Compos Mater Adv Ind n.d. https://nanovia.tech/en/ref/pla-ef/ (accessed June 10, 2024).

[23] Boschetto A, Bottini L, Veniali F. Finishing of Fused Deposition Modeling parts by CNC machining. Robot Comput-Integr Manuf 2016;41:92–101. https://doi.org/10.1016/j.rcim.2016.03.004

[24] International Organization for Standardization. Tool life testing in milling - Part 2: End milling 1989.

[25] International Organization for Standardization. Geometrical Product Specifications (GPS) - Surface texture : Profile method - Rules and procedures for the assessment of surface texture 1997.

[26] Ferraris E, Zhang J, Van Hooreweder B. Thermography based in-process monitoring of Fused Filament Fabrication of polymeric parts. CIRP Ann 2019;68:213–6. https://doi.org/10.1016/j.cirp.2019.04.123

[27] Penu C, Helou M. Acide polylactique (PLA). Tech Ing 2017. https://doi.org/10.51257/a-v1-am3317

[28] International Organization for Standardization. Geometrical Product Specifications (GPS) - Indication of surface texture in technical product documentation 2002.